DØ Note YYYY Draft Version 2

Alignment Strategy for the SMT Disk Detectors

S. Duensing, E. Barberis, and T. Trippe

February 5, 2001

Abstract

This document is written as the SMT disk companion to *Alignment Strategy for the SMT Barrel Detectors*[1]. Much of the barrel document applies equally well to the disks, but we do not duplicate that information. Instead, we refer the barrel document, describing in detail only those issues which are peculiar to the disks or to a combination of barrels and disks.

As with the barrels, the disk alignment process is necessarily iterative. In addition to alignment of disks relative to each other, alignment must be done of disks relative to barrels. It is expected that the iterative process of alignment will extend over the different types of relative alignments (barrel–barrel, disk–disk, and disk–barrel).

This note describes a strategy for determining the alignment of the silicon tracker(SMT) disks, including disk-barrel relative alignments. The sections in this document are parallel to those in the barrel document.

1 Introduction

The disk alignment will proceed in phases similar to that described for the barrels. The first phase is the external alignment using the first modest event sample. In this phase, the entire SMT including disks and barrels can be treated as a rigid body. If a large enough data sample with enough forward tracks is obtained quickly, the relative disk–to–disk and disk-to barrel positions and orientations may also be determined.

The next phase is an internal alignment which uses a minimum of external information. For the forward disks, this might be, for example, track curvature information derived by associating a muon track or electromagnetic cluster with a forward track. The goal for the disks is to refine the relative disk–to–disk positions and the relative wedge–to–wedge positions within a single disk. Once disk–to–disk positions are refined, the dominant degrees of freedom of individual wedges will be allowed to vary, probably first freeing x, then z, in the local wedge frames. As with barrels, the initial disk alignments will have to depend on track samples with isolated hits, later shifting to hit–to–track assignment based on χ^2. Section 3 below discusses the rate of "isolated" tracks in the disks.

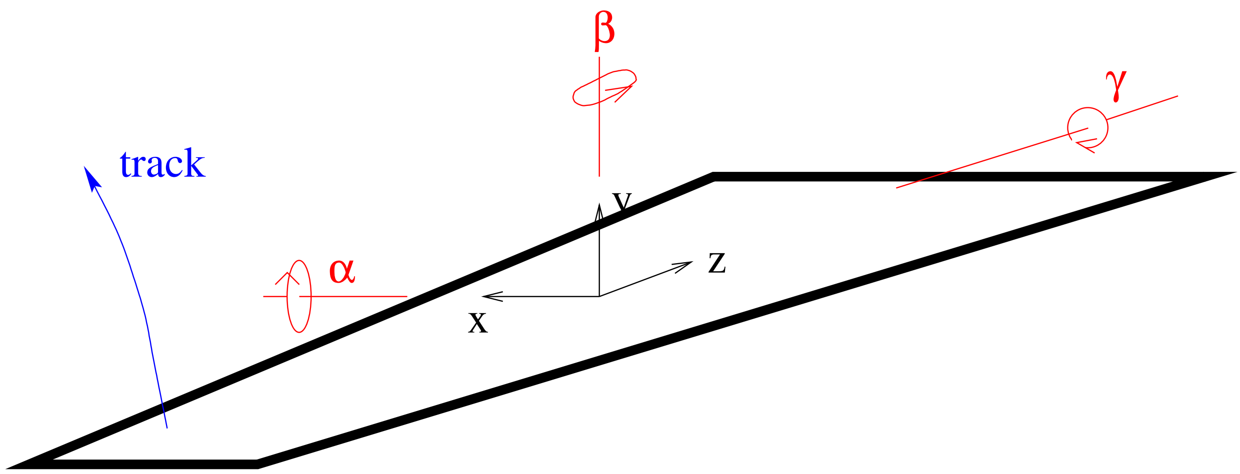

Figure 1: Local coordinates describing wedge positions. Deviations from the nominal position at $x = 0$, $y = 0$, and $z = 0$ are denoted δx, δy and δz respectively. For the ideal geometry $\delta x = \delta y = \delta z = \alpha = \beta = \gamma \equiv 0.0$. The angle ϕ is the angle a track makes with the normal to the wedge in the xy plane, and the angle θ is the angle a track makes with the normal to the wedge in the yz plane. The sign conventions for ϕ and θ follow those of γ and α respectively.

2 Coordinate Systems

As was assumed for ladders, we assume that wedges are perfect planes. We also assume that the individual detectors forming an H–wedge are perfectly aligned[1]. For the alignment, the local coordinate system shown in figure 1 will be used. The relation between the local coordinate system for each wedge and global DØ coordinates for a perfectly assembled detector can be found elsewhere[2]. This has been included in GEANT[3] and in the geometry used in event reconstruction[4]. The H-wedges, though physically made up of single–sided silicon, will initially be treated in pairs by aligning wedge holders, each containing a pair of single–sided H-wedges, rather than the H-wedges themselves. Later, the relative alignment of the H-wedges within a wedge-holder will have to be checked, in particular for the possibility that the two H-wedges could be mounted with a relative stereo angle different than 15^o.

3 Required Alignment Precision

As for the ladders, the target alignment precision for wedges is derived from the condition that alignment errors have a negligible effect on track parameters.

Expected resolutions for barrels and disks are given in DØ Note 3582[5].

The expected resolutions in table 1 vary from pitch/$\sqrt{12}$ because of improvements in resolution due to charge sharing, which in turn depends on track angle (widely varying for

[1]Either of these assumptions can be relaxed as the alignment proceeds. Out–of–the–plane distortions can be accommodate with no change to SMT code. Introduction of misalignment of the individual detectors on an H–wedge will require modest changes to the geometry code.

detector	side	θ_{stereo} (degrees)	pitch (μm)	RMS resolution (μm)	pitch/$\sqrt{12}$ (μm)
ladder	p	0	50	8	14
ladder	n	2	62.5	5	18
ladder	n	90	150	20	43
F-disk	p	15	50	5-10	14
F-disk	n	-15	62.5	?	18
H-disk	p	-7.5	40	12	12

Table 1: Resolutions from DØ Note 3582[5] and pitch divided by $\sqrt{12}$ for each detector and side.

F-disks), Lorentz drift (largest for 0 and 2 degree ladders), and diffusion, largest for the n sides. Noise larger than 10% of the maximum signal could increase the resolution.

We assume the intrinsic hit resolutions of the wedges to be 10 μm in x and 30(70) μm in z for F-disks(H-disks). These are shown in Table 2A, along with the corresponding ladder assumptions from the ladder document[1].

The required alignment precision can be determined using the residual formulas in Section 4.1, which apply to both ladders and wedges. We require that the errors on hit positions increase by no more than 10% when all alignment uncertainties are included. Since there are six alignment parameters, this requirement will be satisfied if each parameter contribute no more than $10\%/\sqrt{6}$ of the intrinsic measurement error. For cases in which the residual term is proportional to a disk or ladder coordinate or a track angle, we assume the average of the absolute value of the coordinate or angle. The assumptions are shown in Table 2A.

Tables 2B and C give the required precision in each alignment parameter. For ladders, the results are roughly a factor of 2 lower than those in the ladder document[1] except for $\delta\beta$, δz, and δy which are 4 to 10 lower. These differences are not yet understood (JOHN, YOU MIGHT WANT TO CHECK THE LADDER ESTIMATES).

If the required precision of a given alignment parameter is quite different for Δx and Δz in Tables 2B and C (*e.g.* β for 2 degree ladders), only the smaller (stronger) requirement is significant. We boldface the significant required precisions in Tables 2B and C, in some cases boldfacing corresponding entries in the two tables if they are nearly equal.

A sample of 600 tracks should yield approximately the precisions shown in Tables 2B and C (assuming that correlations between parameters are small when averaged over the track sample), and even better by a factor of $\sqrt{2}$ when both Δx and Δz contribute equally. This, combined with the fact that at most, four or five parameters are significant (boldface) for Δx or Δz, means that 400 tracks would approximately satisfy the overall precision requirement that errors on hit positions increase by no more than 10%. We assume 600 tracks to be conservative.

A) Assumed resolutions and average track coordinates and angles				
	ladder 2 deg	ladder 90 deg	F-disk	H-disk
σ(x) μm	10	10	10	10
σ(z) μm	350	30	30	70
|x| av mm	8	5	9	11
|z| av mm	30	30	19	35
|φ| av deg	6	6	2	1
|θ| av deg	69	75	10	7

B) Change in parameter to change Δx by (10%/ √6) of σ(x)				
δx μm	**0.4**	**0.4**	**0.4**	**0.4**
δy μm	**4**	4	12	**23**
α mrad	**0.1**	0.1	0.6	**0.7**
β mrad	**0.01**	**0.01**	**0.02**	**0.01**
γ mrad	**0.5**	0.8	1.3	**2.1**

C) Change in parameter to change Δz by (10%/ √6) of σ(z)				
δz μm	**14**	**1**	**1**	**3**
δy μm	**5**	**0.3**	**7**	**23**
α mrad	0.2	**0.01**	**0.4**	**0.7**
β mrad	1.8	0.2	0.1	0.3
γ mrad	0.7	**0.1**	**0.8**	**2.1**

Table 2: Alignment parameter precisions required to limit the induced uncertainties in Δx and Δz to $10\%/\sqrt{6}$ times the resolutions. (A) Assumed intrinsic resolutions $\sigma(x)$ and $\sigma(z)$ and average track coordinates and angles. (B) [(C)] Required alignment parameter precisions based on Δx [Δz].

Summarizing Tables 2B and C, the required precision for the F-disks and H-disks for each of the six alignment parameters defined in figure 1 is:

- δx to better than 0.4 μm
- δy to better than 7(23) μm for an F-disk(H-disk)
- δz to better than 1(3) μm
- α to better than 0.4(0.7) mrad
- β to better than 0.02(0.01) mrad
- γ to better than 0.8(2.1) mrad

These are tighter than is necessary to retain precision on (*e.g.*) the impact parameter because the track parameters average over a set of ladders and wedges.

Ladder Coordinate	*expected Precision* Assembly	Survey
δx	5 μm	5 μm
δy		
δz	5 μm	5 μm
α	40 μrad	40 μrad
β	40 μrad	40 μrad
γ		
Strip Pitch		
Disk–to–disk or barrel		
δZ	50 μm	50 μm
δY	50 μm	50 μm
δZ		
Φ_B		
τ_B	0.4 mrad	0.4 mrad
$\Phi_{B\tau}$		

Table 3: Assembly tolerances and initial survey precision. The angular tolerances were computed using the end–to–end position offsets and the lengths to define an angular tolerance. The coordinates for the ladder–to–ladder section are defined in Figure 1. The coordinates for the barrel–to–barrel section are global DØ coordinates. (THE NUMBERS IN THIS TABLE ARE STILL THOSE FROM THE DISK DOCUMENT. TALK TO VERONICA ABOUT THESE).

The SMT disk assemblies will be surveyed prior to and after installation in DØ. Table 3 gives the expected absolute assembly tolerance, and the precision on the measurements from the assembly survey[6].

4 Residual Formulas

The assembly and initial survey precisions in table 3, imply that the alignment corrections will be small. Given this, residual formulas were derived using small angle approximations of the full transformations[7]. Residuals are defined as the difference between the reconstructed hit position $\vec{x}_{hit}$ and the position at which the interpolation of a track intersects the wedge, $\vec{x}_{track}$. We choose to compute the residual in local detector coordinates (see 2) to simplify the relation between the residuals and alignment parameters. A fully general formulation of multi–dimensional residuals is found elsewhere[8].

As previously mentioned, tracks used in alignment should be determined in a manner to avoid systematic biases [2]

[2]Random effects which increase the residual width but do not introduce bias are acceptable. The resulting wider residual distributions imply, of course, that more data will be needed to achieve the target alignment precision.

(JOHN: IN DISK DOCUMENT, "SYSTEMATIC BIASES" IS MISSING.)
from other detectors.

The situation for the disks is that it is possible to use barrel information to align the F disks with respect to the barrel they are attached to. Using only disk information, the requirement to have at least four (?) disk hits reduces the influence of other detectors to a minimum. The overlap with the muon system is rather small (see discussion of the use of cosmic muons for the disk alignment). Other detectors providing some information about forward tracks are the forward preshower and MIP-muons in the calorimeter. The possible use of this information is not considered here and will probably only be used for alignment of the different detectors with respect to each other.

4.1 Individual Wedges

The hit-track residual in the local coordinate x, called Δx, is given by

$$\Delta x \equiv x_{track} - x_{hit} = \delta x + z \sin\beta + \tan\phi(\delta y + z\sin\alpha + x\sin\gamma) - f(\vec{B}, \phi, \theta) \tag{1}$$

and for the direction perpendicular to this

$$\Delta z \equiv z_{track} - z_{hit} = \delta z + x \sin\beta + \tan\theta(\delta y + z\sin\alpha + x\sin\gamma) - g(\vec{B}, \phi, \theta) \tag{2}$$

Here ϕ is the angle a track makes with the normal to the wedge in the xy plane and θ is the angle a track makes with the normal to the wedge in the yz plane. The functions $f(\vec{B}, \phi, \theta)$ and $g(\vec{B}, \phi, \theta)$ represent systematic uncertainties in the Lorentz-drift corrections for the magnetic non-solenoidal field, and they are odd under reversal of the magnetic field $\vec{B}$. Misalignment is a second order effect in $f(\vec{B})$ and $g(\vec{B})$. For ladders, $g(\vec{B}, \phi, \theta)$ is zero and f does not depend on θ because the in-detector component of $\vec{B}$ is along the z-axis, unlike the disks. The effect of the magnetic field is described in Section 5.3.
****

(ELA AND JOHN. I DO NOT KNOW WHAT THE SECOND ORDER STATEMENT MEANS. PLEASE LOOK OVER THE MAGNETIC FIELD DISCUSSION IN THIS PARAGRAPH SINCE I HAVE TRIED TO MODIFY IT FOR THE DISKS WITHOUT REALLY UNDERSTANDING THE DISK STATEMENTS, A DANGEROUS APPROACH.)
****

The simplest approach to determining the alignment parameters is to use the means of the following histograms(for the Δx case):

1. the distribution of x residuals integrated over x, z (weighted by dn/dz), and ϕ, which gives δx directly, (JOHN: BARREL DOCUMENT SAYS INTEGRATED OVER Y, Z BUT SHOULD SAY X, Z.)

2. the x residual vs. z which gives $\sin\beta$,

3. the x residual vs. $\tan\phi$, integrated over x and ϕ, which gives δy,

4. the x residual/$\tan\phi$ vs. x, integrated over z and ϕ, which gives $\sin\gamma$,

5. and the x residual/$\tan\phi$ vs. z, integrated over x and ϕ, which gives $\sin\alpha$.

measured	misaligned δx	δy	δz	α	β	γ	all	input
δx (μm)	1.029	*	*	*	0.035	1.02	2.35	1
δy (μm)	*	56	*	shape	3	shape	-	57
δz (μm)	*	8.9	7.04	5.13	*	0.13	21.2	7
α $(mrad)$	R	R	R	R	R	R	R	1.6
β $(mrad)$	*	*	*	*	0.0298	0.0077	0.0383	0.0300
γ $(mrad)$	R	R	R	R	R	R	R	5.2

Table 4: The measured H disk misalignments versus the input misalignment. A "*" indicates a measured misalignment within the error, "R" indicates that the effects of a finite resolution make the measurement impossible. "Shape" means that the shape of the distribution is distorted, not (necessarily) the measured result.

While the mean of the track ϕ values is zero this is not the case for θ. For most of the disks, the interaction point will mostly lie on the side towards the origin of the global coordinate system. Thus the θ distribution will have a non-zero mean, which will distort the meaning of (some of) the above mentioned histograms for the z residual.

A simple MC program has been used to check if these histograms give the information and if biases are introduced by the non uniformity of the distributions of tracks in z or by the presence of more than one misalignment. An extensive description of this study and its results can be found in Appendix A.

For the measurement of δx and δz rotations γ or α respectively give a bias. The correlation of x and $\tan\phi$ hide the effect of $\sin\gamma$ in Figure 5. The measurement of α is prohibited by the presence of finite hit resolution (or any other misalignment for that purpose). For the wedges the distribution of tracks in local z is not uniform. A first consequence is that for integrating the distribution of the residuals a weighting of track according to their z has to be done in order to give positive and negative z the same weight. A non-zero $\sin\beta$ term results in a measured δx unless this weighing is done. The correlation of x and $\tan\phi$ in combination with the non-uniform z distribution lets $\sin\gamma$ result in a measured $\sin\beta$. Any rotation is changing the measured δy and the shape of the histogram.

Table 4 summarizes the results of this MC study.

****

THE REST OF SECTION 4 HAS NOT BEEN UPDATED YET. WHAT FOLLOWS UP TO THE BEGINNING OF SECTION 5 IS JUST A COPY OF THE LADDER DOCUMENT AS A PLACE HOLDER. TOM AND ELA AGREED TO DO IT

****

This method, based on the mean of the individual distributions, treats all tracks with equal weight. It should be used if the track errors are systematically biased. It is not understood at what level it matters whether the track parameters used in the residual are computed with or without the using the particular hit appearing in the residual. This is an iterative process, repeated until (*e.g.*) the alignment parameters do not change significantly when an additional pass is made.

When track errors are meaningful and the alignment is known reasonably well, a more comprehensive method is to minimize $\chi^2 \; = \Sigma_{hits}(\Delta x/\sigma_{\Delta x})^2$ as a function of the alignment parameters. Here $\sigma_{\Delta x}$ is the residual error containing terms from silicon hit resolution and track parameter error matrix. In practice, statistics and convergence criteria may imply that not all parameters are allowed to vary simultaneously. Also, the approach in the proceeding paragraph is simply the χ^2 approach in the limit of identical track errors and a sequential minimization for one parameter at a time. A similar expression is used for the Δz calculation.

4.2 Internal Coherent Effects and Further Constraints

In addition to locating the ladder absolution positions using the formulas of section 4.1, it is useful to consider additional means of establishing ladder–to-ladder relative positions using geometrical constraints. The large geometrical ϕ overlap of ladders in adjacent layers automatically introduces ϕ coupling between ladders within a layer. The methods described in this section serve two purposes: (1) tests of systematics arising from the ladder–to–ladder alignment and (2) methods to enhance precision by combining information. It also important to consider whether constraints on the coherent effects give higher intrisic statistical power than individual ladder–by–ladder constraints.

The topologies of particular interest are:

- ϕ correlations using a vertex constraint, and
- effective radius of a barrel layer, to improve the δy precision

4.2.1 ϕ Correlations and Vertex Constraints

The internal alignment described above depends primarily on correlations between ladders at similar ϕ and different radii. The ϕ overlap of "adjacent" ladders in a "layer" introduces a weak coupling between the alignment constants for these ladder and can thus establish the relative position of ladders at very different ϕ positions. An alternate more direct measure can be obtained by introducing a vertex constraint between tracks and computing residuals for tracks fit with this constraint.

If one fits tracks to sets of n_i hits to determine the track parameters (b, κ, ϕ_0) and the position (r_v, ϕ_v) of a vertex common to the tracks, the residuals contain information about the relative positions of the ladders. The vertex constraint implies that the impact parameter b' can be written as a function of the two remaining track parameters and the vertex position.

Given a set of N tracks from a common vertex and denoting the initial 2D track parameters $\{b, \kappa, \phi_0\}_i,\ i = 1, N$, the χ^2 refit of the track under a vertex constraint can be written as

$$\chi^2 = \Sigma_{hits}\frac{r_j^2}{\sigma_j^2} + \Sigma_{tracks}\vec{v}C\vec{v} \tag{3}$$

in which r_j is the residual of the j-th hit to its track, $\vec{v} = (b'(\vec{x}_v, \kappa', \phi_0') - b, \kappa' - \kappa, \phi_0' - \phi_0)$ is a vector of the differences between the original(unprimed) and refit(primed) track parameters and C is the covariance matrix from the original track fit. The function $b'(\vec{x}_v, \kappa', \phi_0')$ is given by a solution to the quadratic form

$$0 = (b')^2 + [\frac{1}{\kappa'} + 2r_v \sin(\phi_v - \phi_0')](b') + r_v[r_v - \frac{\sin(\phi_v - \phi_0')}{\kappa'}] \tag{4}$$

4.2.2 Effective Radius Constraint

An average "radius" of a layer can be determined by assuming the n ladders in a given layer form a regular n–sided polygon. Let δs_i be the difference in local coordinates between hits on two tracks near opposite edges of the same ladder. Further select events such that the hit at smaller ϕ on ladder $i+1$ is on the same track as the higher ϕ hit on ladder i. If the ladders truly formed an n–sided regular polygon, the radius r of the largest circle which can be inscribed in the polygon is related to the δs values[3] by

$$2nr \tan\frac{\pi}{n} = \Sigma_{i=1}^{n} \delta s_i. \tag{5}$$

Let the radius be defined as $r \equiv r_0 + \delta y$ with r_0 the nominal radius and δy the ladder alignment parameter. This is rewritten to give δy as

$$\delta y = \frac{\Sigma_{i=1}^{n} \delta s_i}{2n \tan(\pi/n)} - r_0. \tag{6}$$

The resulting precision is

$$\sigma_{\delta y} = \frac{\sqrt{2}\sigma_{SMT}}{2n \tan(\pi/n)} \tag{7}$$

(JOHN: I THINK THE PRECEEDING FORMULA NEEDS A SQRT(n) IN THE NUMERATOR. NEVERTHELESS I AM NOT ABLE TO GET THE FOLLOWING FORMULA. USING n=12, I GET 7.6/SQRT(N), OR EVEN IF N IS THE NUMBER TRAVERSING ALL PAIRS OF ADJACENT LADDERS, I GET 26/SQRT(N).)
Using the nominal ladder geometry, this gives a precision of

$$\sigma_{\delta y} \approx 50/\sqrt{N} \mu\mathrm{m}. \tag{8}$$

with N the number of tracks traversing a pair of adjacent ladders.

The regular polygon assumption has only a second order dependence on β. This is negligible for all tracks if $\beta < 25$ mrad, or about 0.85 mm difference in radius side–to–side. The effect of the track curving in the gap between layers (or having non-zero impact parameter) giving wrong effective δs will average to zero as long as the geometrical acceptance is unbiased with respect to particle charge and impact parameter.[4]

This should be compared to the precision on δy obtained from the individual ladder method of section 4.1. For that method, the strongest constraint comes from large ϕ_l tracks.

[3] For our geometry, with two sublayers in a single layer, the δs values for ladders in the "outer" radius sublayer must be scaled by the ratio of the nominal radius of the "inner" sublayer to the nominal radius of the outer sublayer.

[4] These can be neglected without resorting to an average by choosing tracks having $p_T > 10$ GeV coming from the primary vertex.

For tracks with $p_T > 5$ GeV crossing an innermost(outermost) ladder at a distance halfway to the edge of the ladder, $\phi_l < 0.18(0.05)$ rad. For this case, $\delta y = \Delta x / \tan \phi_l$. If the mean of the residual is measured to 5 μm and all other effects are negligible, the effective radius is known to 27(100) μm for a ladder in the innermost(outermost) layer.

In choosing which of the two methods to use, there is a trade–off between intrinsic precision and frequency of a specific topology. Both methods will be used, with the more precise result determining the radial alignment constant, and the second method providing a cross–check.

4.3 Barrel–to–Barrel and External Alignment

The previous residual formulas related to the internal alignment of a silicon detector barrel. An alignment to position SMT barrels with respect to each other or to position the SMT with respect to the rest of DØ will also have to be performed. This section gives the residual formulas for positioning the a detector as a rigid body with respect to an external coordinate system corresponding to either a different barrel(barrel–to–barrel) or to the global DØ coordinates(external). Coordinates in capital letters denote an external coordinate system with X, Y, Z cartesian coordinates with Z corresponding to the proton beam direction and X corresponding to a horizontal direction perpendicular to Z and away from the center of the Tevatron. Y is then defined to complete a right–handed system. The tracks used here should not have used the SMT information in determining the trajectory, and residuals for this type of alignment are best expressed in terms of the global system. The residuals for the six rigid body coordinates are:

- For an offset perpendicular to beam, $(\Delta X, \Delta Y) = (\delta R \sin(\Phi - \delta\Phi), \delta R \cos(\Phi - \delta\Phi))$,
- For an offset along beam, $\Delta Z = constant$,
- For a rotation about nominal beam axis, $\Delta\Phi = constant$
- tilt of angle τ with respect to beam axis making an angle $\delta\Phi_\tau$ in (R, Φ) plane, $(\Delta X, \Delta Y) = (Z \sin\tau \sin(\Phi - \delta\Phi_\tau), Z \sin\tau \cos(\Phi - \delta\Phi_\tau)$.

5 Data Samples and Rates

Having established the required alignment precision and the residual formulas for the disks, the data samples used to perform the alignment are now considered. The effect of the solenoid field on the alignment strategy is also discussed.

5.1 Cosmic Ray Muons

The total muon cosmic ray flux[5] at sea level is $\approx 0.02/\text{cm}^2/\text{s}$, with an angular distribution $\propto \cos^2\theta_a$[10]. Here θ_a is the muon angle with respect to vertical. For aligning the disks with respect to each other without using any non-disk hits, tracks with at least 4

[5] There is a charge asymmetry of 1.25 μ^+ for every μ^-.

disk hits are needed. In the following pictures of the disk layout and muon detector inner edge along the dotted beam line, one can see all the angles from which a cosmic μ has to come in to at least leave a hit in the muon detector and in the outer/inner H/F disk re shown.

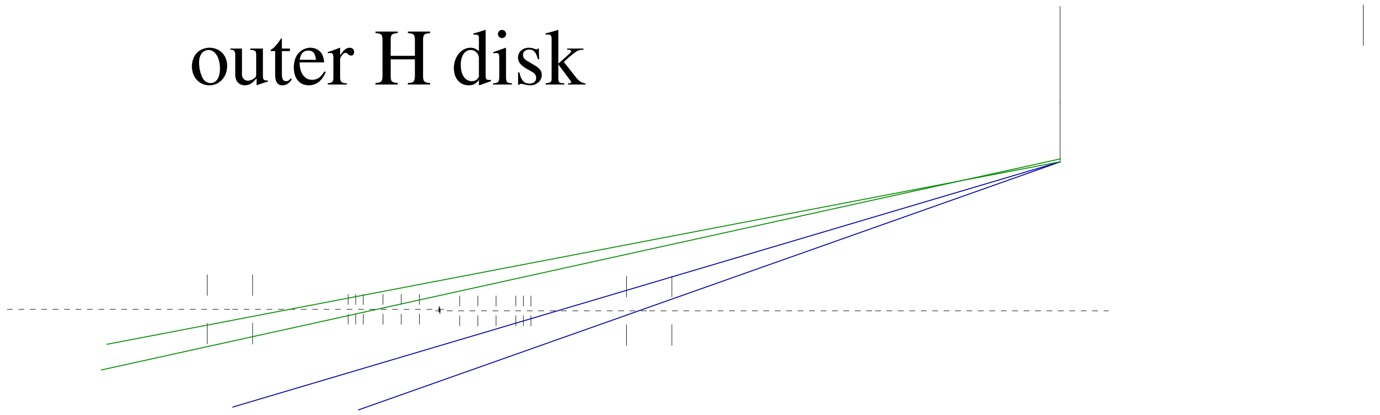

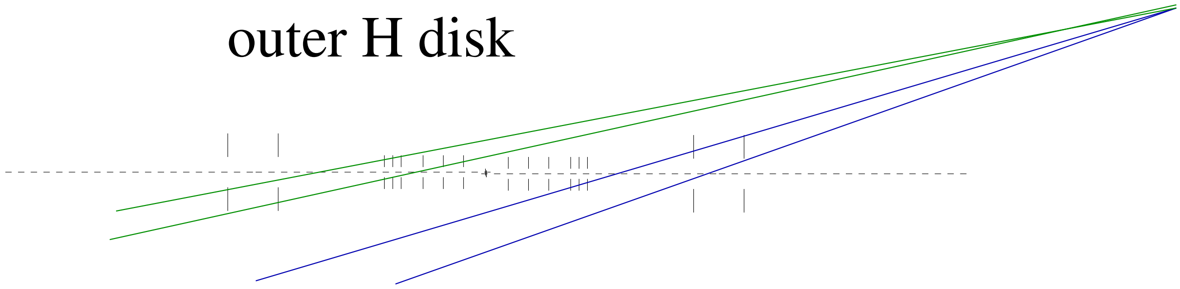

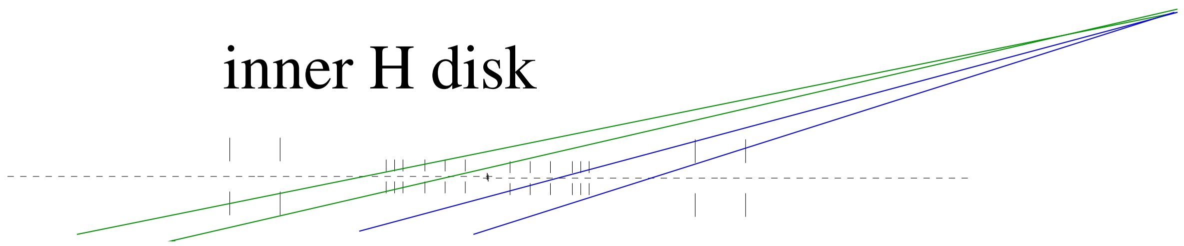

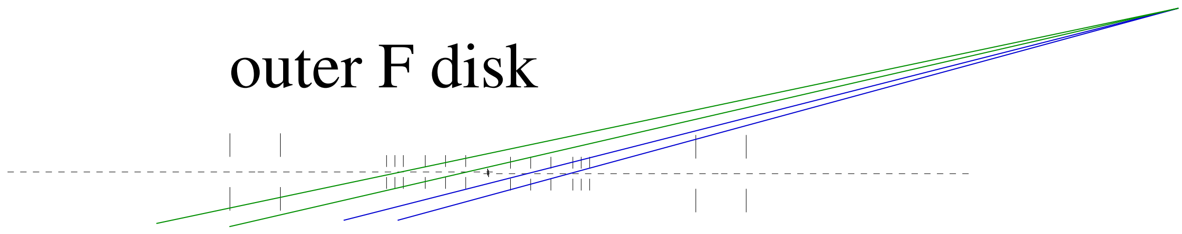

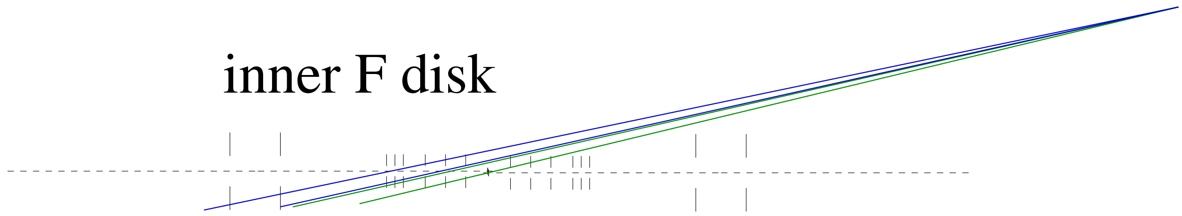

As can be seen, for the outer H-disks, inner H-disks, and F-disks it could be possible to use cosmic muons. This is only valid for a dedicated cosmic run where a single trace of a muon in the detector already causes the event to be written to tape.

Cosmic muons can be used to align the F-disks with respect to the barrel. The θ angles a track has to have for this task are given in table 5. Considering only μ's which pass within 2 mm of the nominal beam line[6], the integrated muon rate for the F disk wedges is given in table 5.

5.2 Minbias and p_T Selection

For the alignment of the disks with respect to the barrel the rate estimates for the rather should not differ that much from the rates given in the corresponding section of the barrel document, at least as far as the F disks are concerned.

For the alignment of the disks with respect to each other without using any barrel information the tracks that can be used will have a much larger */eta*. What matters in order to reduce multiple scattering effects will be using high p tracks rather than requiring a high p_T which would reduce that rate very much.

Collider data will also be used for alignment. At design luminosity, the rate from $W \to e\nu$ and $W \to \mu\nu$ will be 2 hz total or roughly 0.02 hz per four ladder tower. These events will provide slightly better statistical precision than cosmic ray muon data, and the flat ϕ distribution gives all ladders equal statistical weight. They also have high p_T tracks thus

[6]The currently planned triggers have a strong bias to particles passing near the beam line. Relaxing this would allow additional handles for alignment and should be considered.

F Wedge position		Rate	
Disk	z position (cm)	ϕ (degrees)	(10^{-3} hz)
1		0	x
2		0	x
3		0	x
4		0	x
5		0	x
6		0	x
		15	x
		30	x

Table 5: Cosmic ray rates for specific wedges. The computation required the particle to pass within 2 mm of the beam line and to have at least one F disk hit. The column labelled ϕ gives the azimuthal angle of the center of the wedge in DØ global coordinates.

minimizing multiple scattering effects, for the disks what matters for that rather that high pt is a high p.

Higher statistics samples can be obtained from minimum bias (or jet) triggers. The tracks in these events have falling p_T distributions, so a trade off between rate and multiple scattering effects will occur. The lower p_T tracks have broader residuals and thus the precision of the measurement of the residual mean is lower. The cross–over between resolution dominated by multiple scattering and resolution dominated by measurement errors occurs at $p_T \approx 4$ Gev (p_T -¿ p?).

5.3 Effect of the magnetic field

A shift in the distribution of hit residuals could be due either to a misalignment or to an incorrect calibration of the Lorentz drift of electrons/holes under magnetic field, or to the combination of both. Given that the Lorentz drift arises from the component of the magnetic field which is perpendicular to the electric field applied to the sensor, and given that the solenoidal field has nearly zero radial component in the inner region of the silicon tracker, the Lorentz drift for the F disks is negligible, while non zero values of B_r start to give an effect in the H disks.

Figure 2 shows the value of B_r as a function of z, for several values of r. The values of B_r have been extracted from a calculated field map (i.e. as contained in the current GEANT simulation); preliminary data confirm the accuracy of such calculation. The value of B_r in the F disks region ($z < |50|$ cm) is < 0.012 T, translating into a shift of $< 0.2\mu$m and therefore negligible. The value of B_r at the position of the inner(outer) H disks, 94(126) cm, translates into a maximum shift (at the outer edge) of $0.6(1.2)\mu$m. The shift is, at maximum, of the order of 10% the expected resolution, averaged over track angles, but care should be placed into calibrating field effects in that region, since it is a region of non-uniformity.

The best strategy for achieving a field-independent alignment w.r.t. to the disks will be to perform two alignments with the field reversed between the two data sets. The option

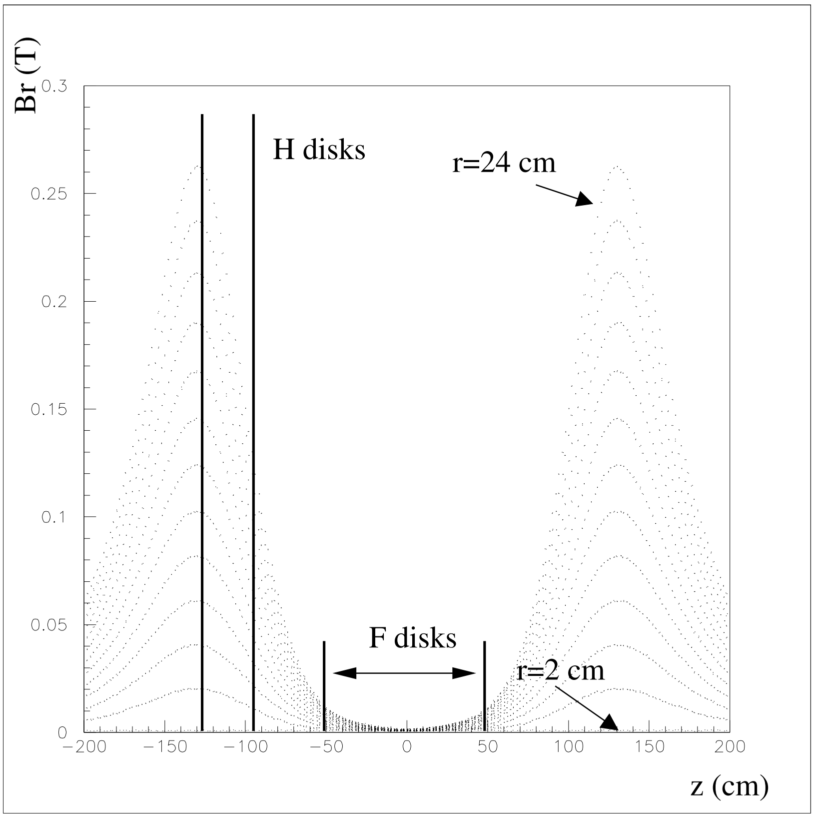

Figure 2: B_r as function of z for different r values (from 2 to 24 cm in steps of 2cm), indicated are the range in position for the F disks and the position of two of the H disks, the remaining ones being symmetric in z

of performing alignment with the field turned off is unattractive because of the inability of bending away low p_T background tracks.

6 Approximate Time Scales

(THIS SECTION IS UNCHANGED FROM THE LADDER DOCUMENT EXCEPT FOR REMOVAL OF THE SECOND PARAGRAPH. IT STILL NEEDS TO BE DONE.)

Given the information above, the time it takes to complete the first two phases of the alignment can be determined. The calculations use the expected initial survey precision and target alignment precision (section 3), the data rates (section 5), and assume the alignment precision is determined by the error on the mean of the residual distributions. This error depends linearly on the width of the residual and has the usual $1/\sqrt{N}$ statistical dependence. However, the width of the residuals will depend somewhat on the initial alignment precision. We take the expected initial values to compute the residual widths.

If the initial luminosity is low, or we have time for cosmic ray running, this step of the alignment will be performed using cosmic rays. The asymmetry in global ϕ of cosmic rays implies that the time needed depends on $\delta\Phi$. The time is maximized if the misalignment has $\delta\Phi = 90^o$ (a shift in global y), and minimized if the misalignment has $\delta\Phi = 0$ (a shift in x). The crude calculation given here assumes the worst case shift $\delta\Phi = 90^o$ and that only tracks which pass through the innermost ladders at $\phi = 60^o,\ 120^o$ are used. This was chosen for simplicity with the understanding that the ladders at $\phi = 90^o$ contribute very little for the worst–case shift, and that the rate through the ladders near $\phi = 0$ is extremely low. Of course, data through all ladders will be used, so the time here is an overestimate. The exposure time T is approximately

$$T = \frac{N_T}{N_B * 2 * \cos(\phi) * R} = \mathbf{30} \text{ minutes}$$

Here $N_T = 200$ is the number of tracks required, $N_B = 6$ is the number of barrels, R is the rate through a single ladder at ϕ, and the factor of two arises because detector symmetry implies there are ladders at ϕ and $\pi - \phi$. Establishing the same set of constants for each barrel requires a factor of six increase in data.

The internal ladder–to–ladder alignment target precisions are given in section 3. If we assume that the tracks used for the internal alignment have SMT information with geometrical information at the precision expected from the survey, the residual width will be less than 15 μm for the axial sides and less than 45(550) μm for the rz $90^o(2^o)$ stereo sides. This implies that 3000 $p_T > 5$ GeV tracks per ladder are [7] are required to achieve the target precision in each variable. The residual width is taken as the quadrature sum of the hit resolution and track position uncertainties. We assume that the data are split between opposite polarities of the field, allowing cancellation of the Lorentz drift effect in the residuals. Table 6 gives the exposure times for cosmic ray and collider data samples.

[7] If the magnet–off method is used, the p_T selection cannot be made, and all isolated tracks will be used. This implies that multiple scattering will increase the width. For 1 GeV tracks the resolution is a factor of three worse than for 5 GeV tracks. The track p_T based triggers will not work. For cosmic ray data this is not a problem, but for collider data, a different trigger scheme would be needed.

Sample	Time (days)
Cosmics, Inner Layer, $\phi = 0$	7
Cosmics, Inner Layer, $\phi = 60^o$	2
Cosmics, Outer Layer, $\phi = 7.5^o$	30
Cosmics, Outer Layer, $\phi = 67.5^o$	2
Minbias Collider Data ($p_T > 5$ GeV)	0.3
$W \to (e, \mu)\nu$	3

Table 6: Exposure time needed to achieve the desired alignment precision for the first pass internal alignment. The minbias results assume constant $dN/d\eta$ for tracks within $|\eta| < 1.6$ and 20 hz trigger rate (a prescale of 15 on the physics rate at design luminosity). The times given are to accumulate enough data to align all ladders including the factor of two to allow for reversed field running. Each track is assumed to traverse four layers.

7 Summary

(THIS SECTION IS UNCHANGED FROM THE LADDER DOCUMENT. IT STILL NEEDS TO BE DONE.)

A method to align the SMT ladders has been described, including the evolution in methods as the data sample increases and the alignment precision improves. It is found that an initial alignment of the entire SMT with the rest of DØ requires less than one day of cosmic ray data. A precision alignment of the ladders will require less than a week of cosmic ray running or collider running at design luminosity. The collider rates are based on saturating trigger bandwidth using dedicated or physics triggers. These results assume data is taken with two opposite polarity settings of the DØ solenoid in order to cancel Lorentz drift effects, and that only isolated tracks are used. The numerical results presented here will be updated based on detailed Monte Carlo studies to be performed over the next six months.

A Appendix A

A.0.1 The Toy MC

The used coordinate system is deducted from the local coordinate system of a wedge (ladder). x and z are used as defined before and y is perpendicular to the detector element (in “beam” direction). This toy MC approximates tracks as straight lines (high momentum limit). The origin of the track is smeared with a gaussian in all coordinates, the distributions are shown in Figure 3. The tracks are either propagated to a pseudo ladder which is perpendicular to the “beam” direction where the middle of the pseudo ladder sits at x=z=0 or to a H wedge which sits at its nominal position with respect to the beam line. The tracks are projected to y=126 cm (nominal position of the outer H disk) and the residuals are computed according to formulas (1) and (2) using the x and z the tracks would have at the nominal wedge/ladder position. The calculated residual is then smeared with a hit resolution of 10 μm. The residual before and after smearing are used to make the histograms described in Section 4.1.

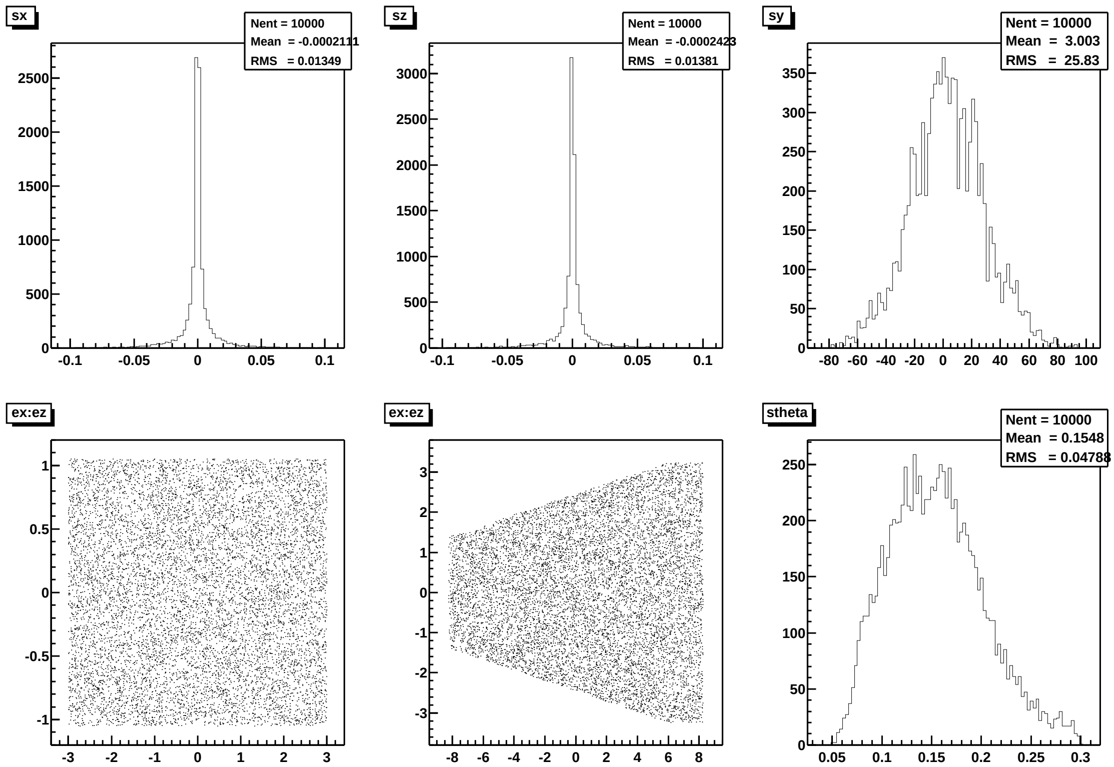

Figure 3: Distributions for start xyz values (upper plots) and the endpoints in xz for the pseudo ladder and the H wedge (lower left and middle). The lower right plot shows the θ distribution for H wedges resulting from the input distribution and the shape of the wedge.

Every parameter is varied alone, all of them at the same time and all except for the one that should be measured by the considered histogram. The parameters are shifted by the maximal allowed misalignments (as given in Table 2) for the H Wedge, these values are used for the pseudo ladder as well.

A.0.2 Results for the Pseudo Ladder

δx: the distribution of x residuals integrated over y, z, and ϕ

The mean of the distribution of the x residuals in Figure 4 is shifted by δx as expected. A non-zero $\sin\gamma$ produces an effect as well. The contribution of γ to Δx is $\tan\phi\ x\ \sin\gamma$. Due to the correlation of $\tan\phi$ and x it is of the same sign as $\sin\gamma$.

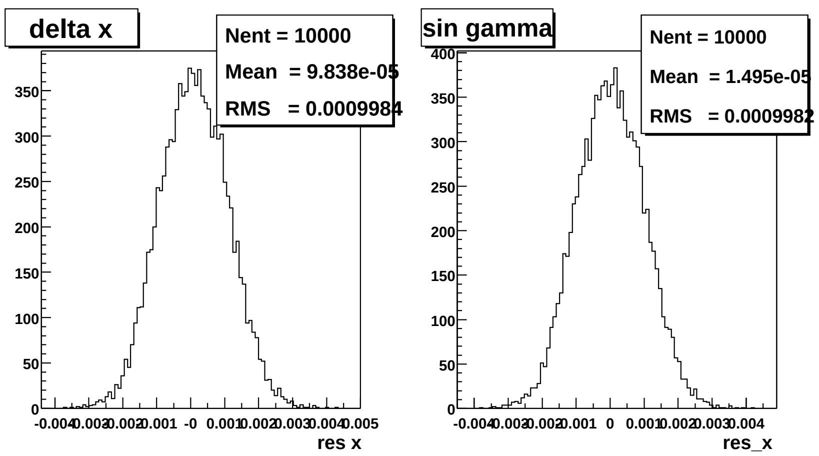

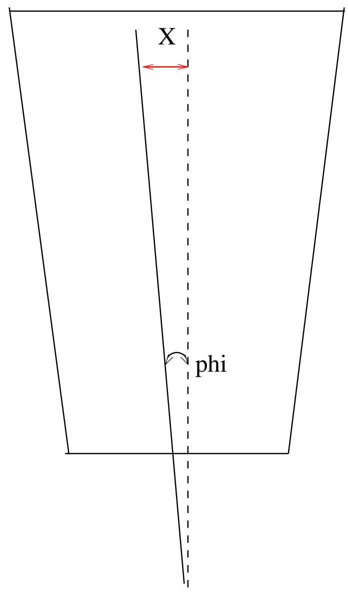

Figure 4: Distributions of Δx for only δx (left) and only γ (middle) misalignments. The right figure illustrates the correlation of x and $\tan\phi$. SILKE, IS THE PHI IN THE RIGHT HAND FIGURE THE SAME PHI AS GIVEN IN THE CAPTION OF FIGURE 1 OF THIS REPORT AND USED IN THE RESIDUAL FORMULAS? IT DOESN'T LOOK LIKE IT.

sin β: Δx vs. z

Figure 5 shows the profile histogram of the x residual versus z for 10000 tracks where all parameters have been varied, among those $\sin\beta$ by 0.03 mrad.

δy: Δx vs. $\tan\phi$

The shape of the profile histogram of x residual versus $\tan\phi$ with all parameters misaligned is a result of the shift in δy and $\sin\gamma$ as can be seen in Figure 6. $\sin\beta$ can still be extracted as the average of the left and right rise:

$$m_{left} = m_{\delta y} - |m_{\sin\gamma}|$$
$$m_{right} = m_{\delta y} + |m_{\sin\gamma}|$$
$$m_{\delta y} = (m_{right} + m_{left})/2$$

The result for 10,000 tracks with an assumed hit resolution of 10 μm is 218 $\pm$ 41 μm instead of the expected 57 μm, for 500,000 tracks the result is within the errors (61 $\pm$ 6 μm).

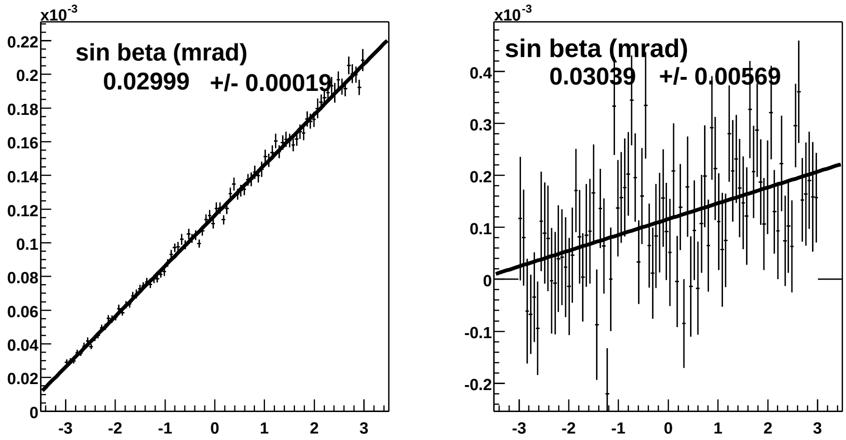

Figure 5: Profile histograms of Δx versus z, where both the vertical (Δx) and horizontal (z) axes have centimeter units. The assumed hit resolutions are 0 (left) and 10 (right) μm.

$\sin\gamma$**: $\Delta x/\tan\phi$ vs. x**
Due to the large correlation of x and $\tan\phi$ this histogram is of no use, unless only $\sin\gamma$ is non zero and the hit resolution is zero. This is illustrated in fig 7.

The fact that $\sin\gamma$ cannot be easily extracted from a histogram means that one cannot correct for the effects a non-zero (or unknown for that matter) $\sin\gamma$ has for the extraction of other parameters.

$\sin\alpha$**: the $\Delta x/\tan\phi$ vs. z**
Non-zero x residuals introduced either by finite hit resolution or other misalignments make the measurement of $\sin\alpha$ via this histogram impossible as can be seen in Figure 8. More statistics (increasing the sample from 10,000 tracks to 500,000 tracks does not change this situation.

A.0.3 Results for the H Wedge

The histograms of which the results were not useful in the case of the pseudo ladder didn't do it in the case of an H wedge either. Thus only the cases where the parameters could be extracted in the case of the ladder will be considered and additional problems introduced by the shape of the wedge/non-uniformity of the θ distribution will be discussed.

δx**: the distribution of Δx integrated over y, z, and ϕ**
The effect of a non-zero γ is the same as described for the ladder.

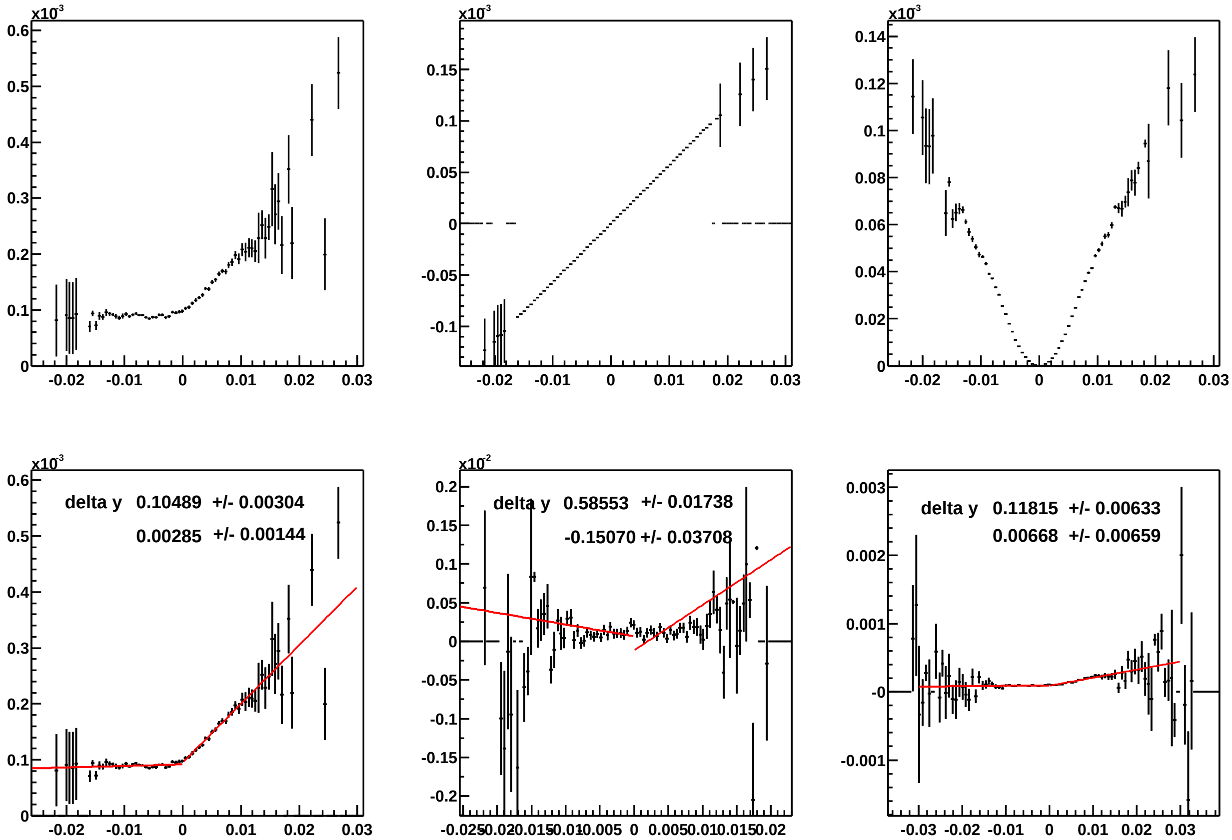

Figure 6: Profile histograms of Δx versus $\tan\phi$ (10,000 tracks). The shape of the profile histogram where all parameters have been misaligned (upper left) is a result of the shift in δy (upper middle) and $\sin\gamma$ (upper right). The lower plots show the results of the fit to two straight lines, assuming resolutions of 0 (left) or 10 μm (middle and right) and increasing the statistics in the right plot to 500,000 tracks.

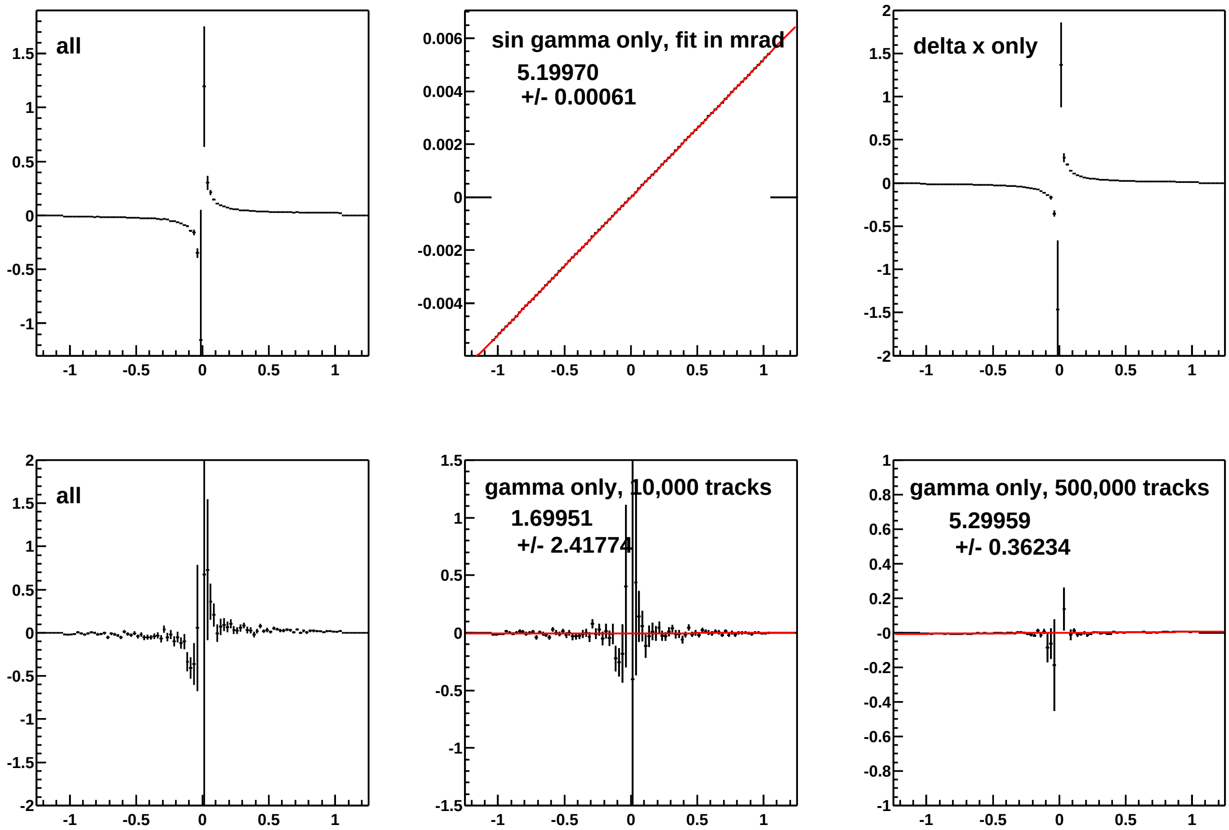

Figure 7: Profile histograms of $\Delta x/\tan\phi$ versus x. The upper plots assume a hit resolution of 0 μm, all parameters (left) only γ (middle) or only δx (right) are misaligned. For the lower row of plots the hit resolution is set to 10 μm. All parameters are misaligned (left), otherwise only γ is non zero, the right plots contains 500,000 tracks.

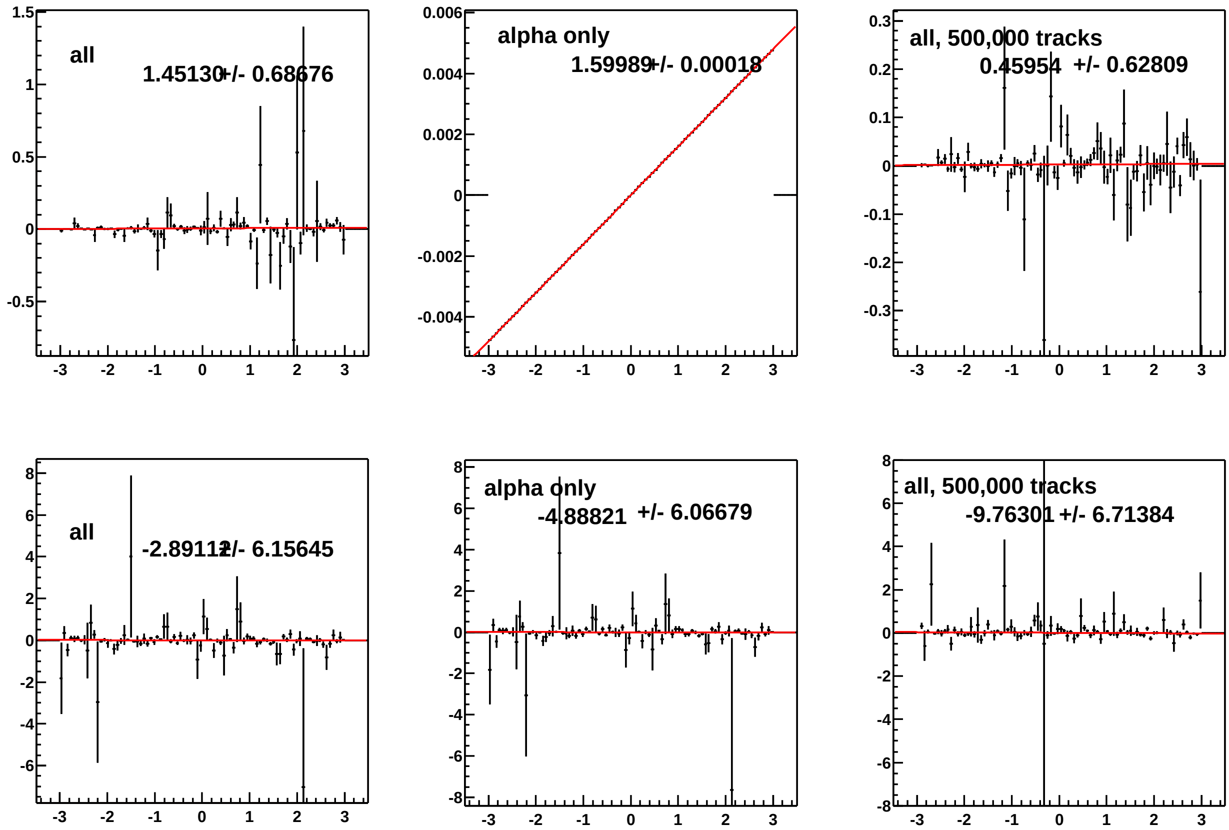

Figure 8: Profile histograms of $\Delta x/\tan\phi$ versus z. An ideal hit resolution has been assumed for the upper plots and 10 μm for the lower ones. In the left and right plots all paramters are misaligned, in the middle only α is changed.

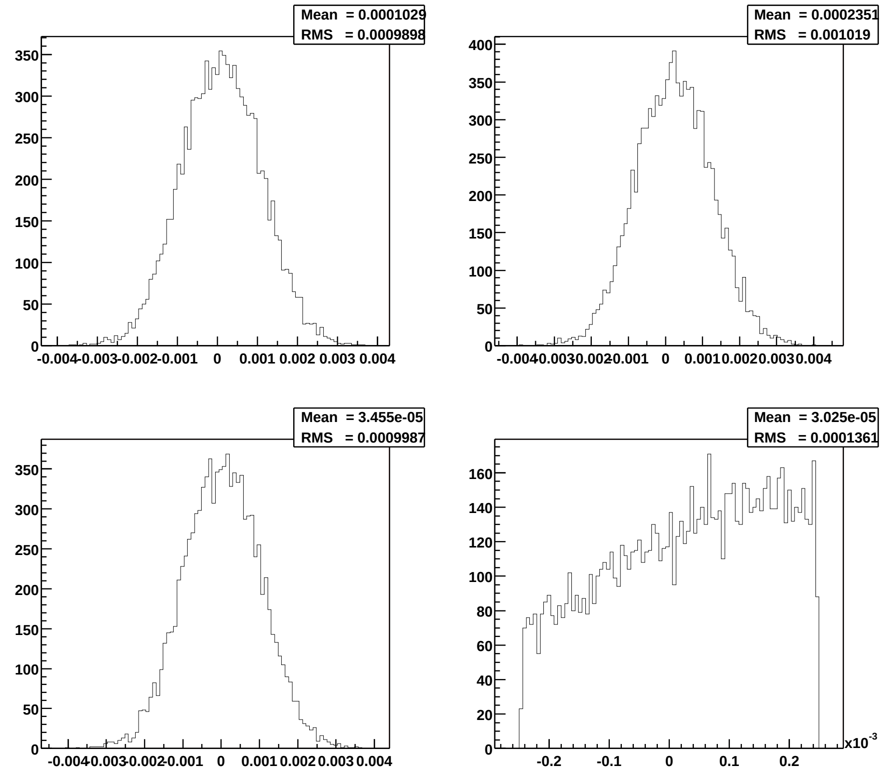

The upper right plot shows the Δx distribution with only δx not equal to zero, for the upper right plot all parameters have been varied and for the lower left plot only β. The lower right plot shows the β effect for a hit resolution of 0.

The $z \sin \beta$ in equation (1) causes a shift in the mean of the δx distribution unless the tracks are given a weight to correct for the non-uniformity in z.

Figure 9: Δx integrated over x, z, ϕ and θ

The effect of $\sin \gamma$ is as big as the effect that one wanted to measure in this case, and thus one has to be careful about using this histogram unless one either knows γ or at least knows that it is small enough for its effect to be negligible.

$\sin\beta$**:** Δx **vs.** z

In the case of a wedge γ has an effect on the histogram as can be seen in Figure 10. A hit resolution of 10 μm is assumed for this plot. For the upper left plot all parameters are varied, only β is set to 0.03 mrad for the upper right plot and only γ is set to 57 mrad in the lower left plot. $\Delta x \propto \tan\phi x \sin\gamma)$ and $\tan\phi x$ is (nearly) always positive. Due to the shape of the wedge the range for $\tan\phi x$ is higher for higher z as the wedge is wider, thus the average $\tan\phi x$ gets bigger with increasing z. SILKE: YOU COMMENTED THAT THE TEXT IS WRONG HERE BUT I COULD NOT FIGURE OUT HOW TO FIX IT FROM YOUR COMMENT. COULD YOU REWRITE IT FOR ME.

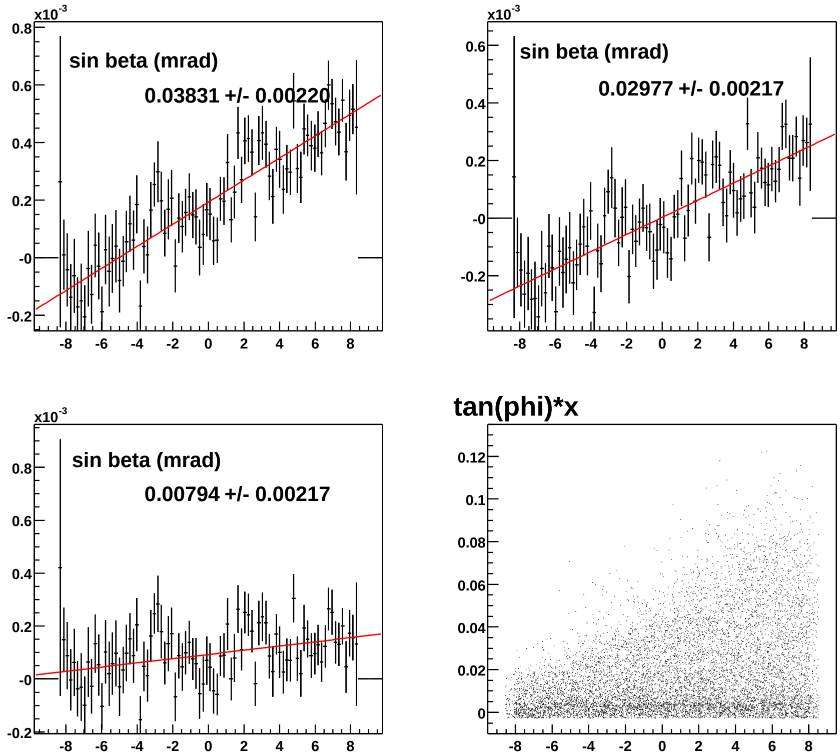

Figure 10: Profile histogram of Δx versus z

δy**:** Δx **vs.** $\tan\phi$

The effect of γ is the same as seen for the ladder, this effect can be taken out in the same way as described there.

The effects of α and β are due to the shape of the wedge. $\tan\phi$ is directly correlated to x and thus to z. For $x < x_{min}$ positive and negative z values are equally likely, for bigger x values z get more and more positive on average. This explain the shape of the effects caused by α and β, the α term ... is uneven and will cause a net effect while the β term should disappear when making two fits like the γ. In Figure 12 the effect of a finite hit resolution and statistics is illustrated.

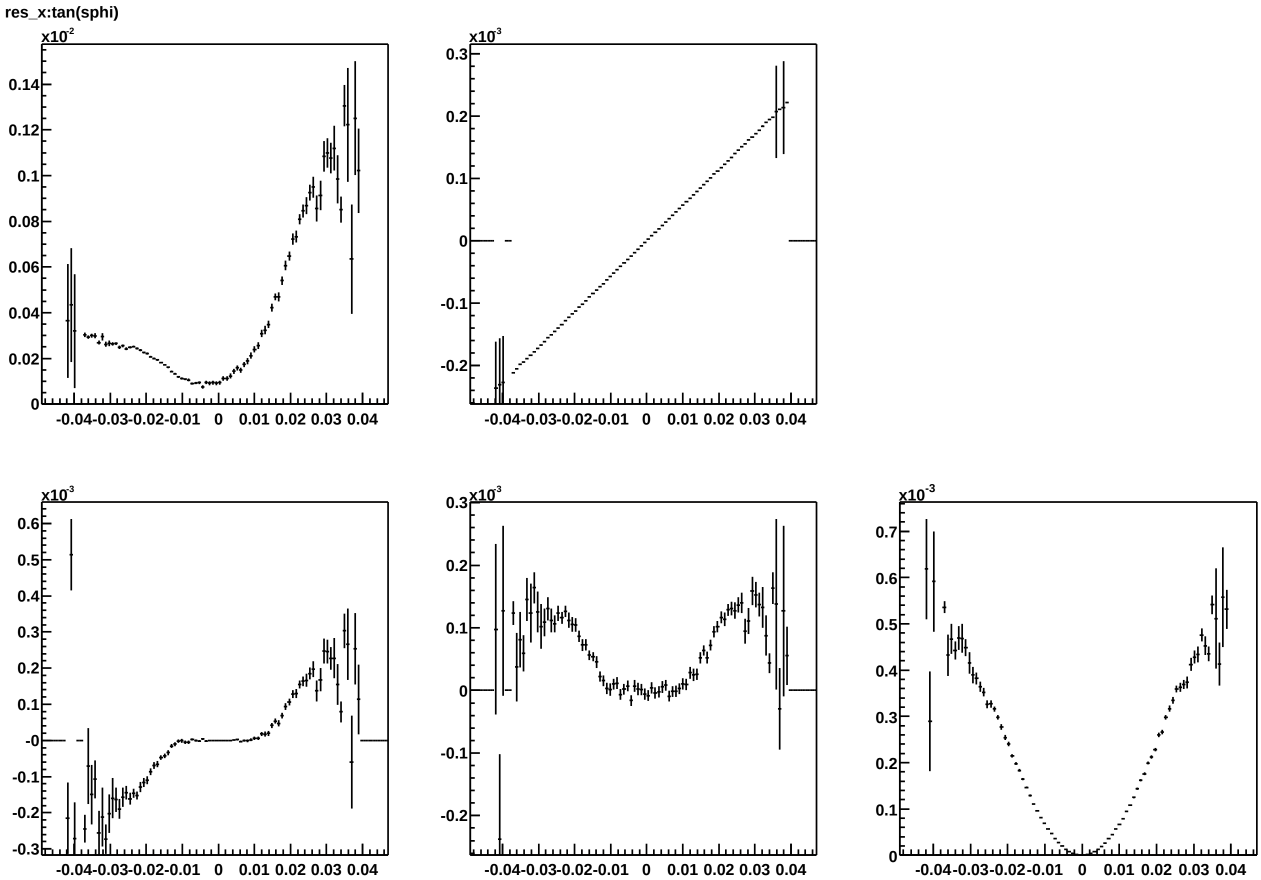

Figure 11: Profile histogram of the x residual versus $\tan\phi$. An ideal hit resolution was assumed, varied were all (upper left), δy (upper middle), α (lower left), β (lower middle) and γ (lower right).

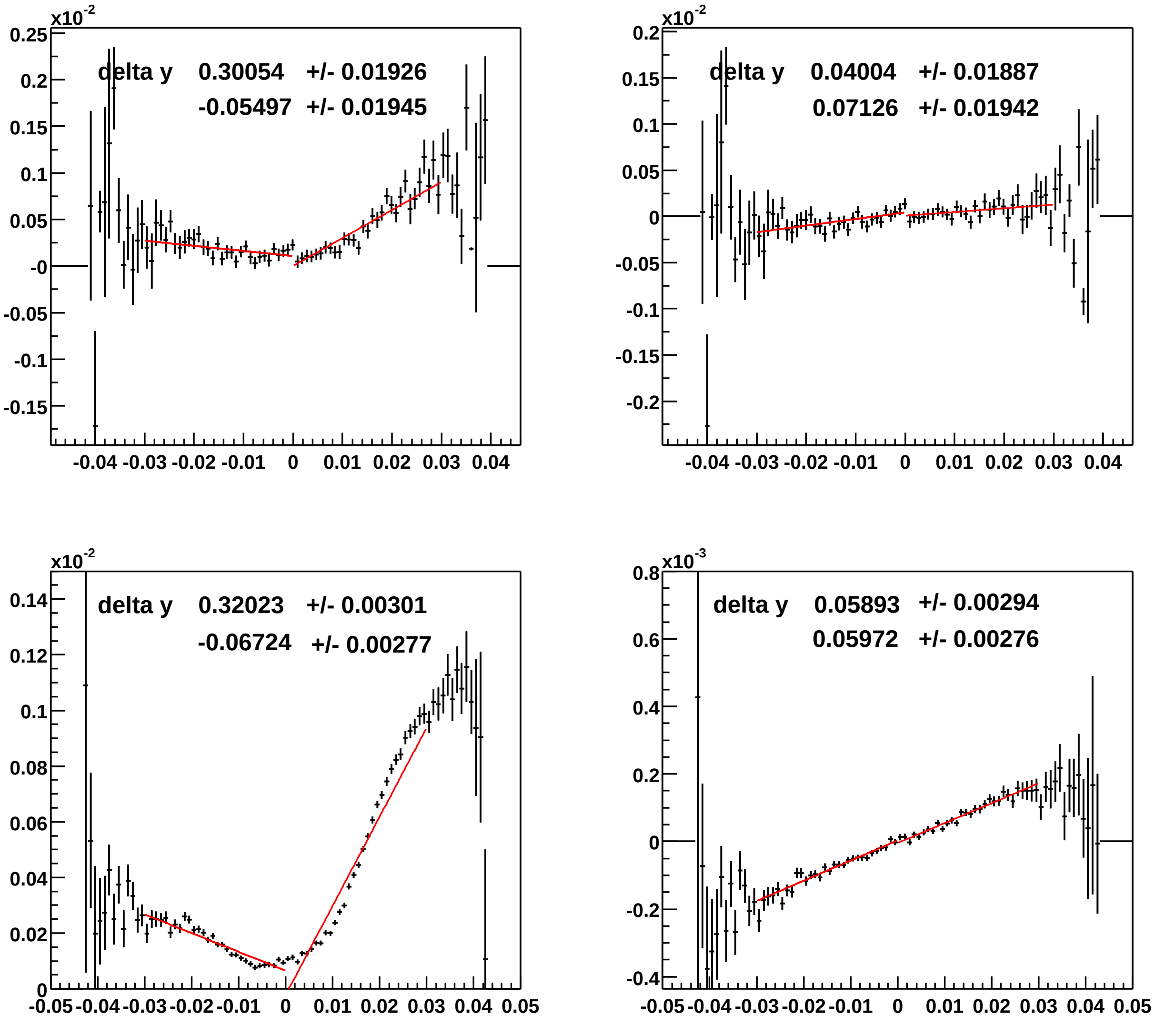

Figure 12: The upper plots contain 10,000 tracks, the lower 500,000. The parameters considered are all for the left plots and δy for the right ones.

References

[1] *Alignment Strategy for the SMT Barrel Detectors*, D. Chakraborty and J. D. Hobbs, DØ Note XXXX, `http://d0server1.fnal.gov/projects/OfflineCalibAlign/docs/alignment/smtbar01.ps`

[2] See `http://www-d0.fnal.gov/~meena/d0_private/silicon/coords/smt-numb/sld001.htm`

[3] *Geant Simulation of the DØ Silicon Microstrip Tracker*, M. Narain, B. Pawlik.

[4] `http://www-d0.fnal.gov/d0dist/dist/packages/silicon_geometry/devel/doc`

[5] *H-Disk Accuracy and Position Revisited*, M. Kubantsev, N. Reay, E. Shabalina, DØ Note 3852 (Jan. 13, 1999).

[6] Private Communication, Bill Cooper.

[7] See *Mechanics*, H. Goldstein, 2^{nd} Edition, Addison Wesley. The small angle forms of transformations are in section 4-8. The roll, pitch, yaw coordinate system and the resulting rotation matrix are described in Appendix B.

[8] *Visual Alignment: 3D Residual Formulas; Silicon Microtracker Examples*, 9/3/99 draft, available at `http://d0lblt.lbl.gov/wwwtrippe/VisualAlignment.ps`.

[9] DØ Note 3636, Y. Gershtein.

[10] The basic information used here comes from section 21 of *Particle Physics Booklet*, extracted from *Review of Particle Properties*, C. Caso, *et. al.*, Eur. Phy. J. **C3**(1998) 1.